Received: 16 June 2020 | Revised: 17 September 2020 | Accepted: 22 October 2020

IET Generation, Transmission & Distribution

DOI: 10.1049/gtd2.12065

The Institution of Engineering and Technology WILEY

ORIGINAL RESEARCH PAPER

Proactive repair crew deployment to improve transmission system resilience against hurricanes

Yiheng Bian | Zhaohong Bie | Gengfeng Li

The State Key Laboratory of Electrical Insulation and Power Equipment, Shaanxi Key Laboratory of Smart Grid, Xi'an Jiaotong University, Xi'an, China

Correspondence
Zhaohong Bie, The State Key Laboratory of Electrical Insulation and Power Equipment, Shaanxi Key Laboratory of Smart Grid, Xi'an Jiaotong University, Xi'an 710049, China.
Email: zhbie@mail.xjtu.edu.cn

Funding information
Science and Technology Project of State Grid, Grant/Award Number: 5202011600UG

Abstract

Extreme weather events, such as hurricanes, impose severe impacts on power systems. A rapid repair for power systems is desired after hurricanes pass to mitigate load-shedding losses. This study proposes a proactive repair crew deployment model to prepare for post-disaster repair and restoration. A two-stage stochastic optimisation framework is designed. In the first stage, the repair crews are allocated to candidate locations ahead of a hurricane. In the second stage, the repair dispatch and load restoration are implemented under several damage scenarios to support the first-stage decision-making. A novel repair crew routing method is proposed which considers repair crew cooperation on important damaged components to enable earlier restoration of critical load. A linear-programming approximation of AC power flow is applied to model the restoration of the transmission system in which the generator start-up characters and security constraints are incorporated. A scenario-based decomposition algorithm is applied to solve the stochastic problem and a preprocessing method to identify necessary components is proposed to further reduce computation time. Case studies validate the effectiveness of the proposed model in improving transmission system resilience.

1 | INTRODUCTION

Modern society highly relies on a stable and reliable power supply. Most present power systems are designed in a way that they have the ability to resist typical threats but are vulnerable to the low probability but high-impact extreme weather events. In 2017, hurricanes Harvey, Irma, and Maria successively struck the power systems, and each caused power interruption of more than one million consumers [1, 2]. Under a hurricane, the overhead transmission lines are subjected to extreme wind and flying debris. What is worse, hurricanes and concurrent rainstorms can bring a large-scale flood to coastal and riverine areas, resulting in a high probability of the equipment in substations located below the base flood elevation to suffer from inundation, erosion, scour, and wave action [3].

Despite their severe impacts, most wind-related weather disasters can be predicted 24–72 h in advance [4], which makes it possible for utility companies to prepare in advance. Several researches have been done in the context of proactive preparedness. Authors in [5] developed a bi-level stochastic response model for the interdependent traffic-electric system to assign mitigation actions and repair resources before hazards to maximise the expected functionality. In [6], an adaptive robust pre-disturbance-scheduling model is proposed for microgrids to mitigate the power interruption risk in face of weather disasters. The authors in [7] allocate generation resources including diesel oil and batteries in distribution systems ahead of a hurricane to serve critical load in post-hurricane restoration. A proactive generation re-dispatch strategy before and during extreme weather events is proposed in [8]. The operating strategies are established considering both the current and potential future component status as the extreme event-unfolding through a Markovian method. Relevant literatures mainly focus on resources allocation and system pre-scheduling. The deployment of repair crews, which can enable a faster repair especially for transmission system components far from the utility companies, has been rarely studied.

In the topic of repair crew dispatch, a co-optimisation model which coordinates repair and service restoration is established in [9], where the repair dispatch and power operations are

coupled with each other through damaged component status. The authors in [10] further developed the co-optimisation model by incorporating the dispatch of mobile power sources and applying vertex-wise variables to model the repair crew's routing problem. In [11], the authors coordinated the line and tree crew dispatch as well as carry resource for an unbalanced distribution system. The routing solution can be updated as more information is obtained to tackle the repair and demand uncertainties. In [12], the combined repair and restoration problem for interdependent power and natural gas systems are studied. The effect of depots location on improving repair efficiency is also validated. The authors in [13] investigated the repair-dispatching problem in the context of the transmission system. The accuracy of DC and linear-programming approximation of AC power flows (LPAC) model are compared, which reveals the necessity to model the reactive power and voltage magnitudes in transmission system restoration problem. Most existing researches on power system repair dispatch assume that each damaged component is repaired by only one of the crews [9, 10, 12]. However, this limitation may yield sub-optimal results compared to allowing multiple crews to collaboratively repair one component for the reasons that: (1) Some critical components should be repaired as soon as possible and the cooperation of multiple crews can speed up the repair progress, (2) the crews completing their assigned work can proceed to support other teams rather than return to depots directly. Authors in [14] proposed a dynamic routing model where a new crew can join the repair process of one component at any time and accelerate the remaining repair. They establish a recurrence formula to cumulate the progress of participating crews and use an inverse function to represent the remaining repair time. However, this approach inevitably imposes a computational burden. In this study, we propose a more computationally efficient crew routing method in which the collaborative repair to speed up the repair process is considered.

In the topic of power system restoration, Sun et al. [15] divided transmission system restoration into three stages: Generator start-up, transmission line restoration, and load restoration. A major concern is to ensure the power flow feasibility during the restoration. In [16], the authors proposed an optimal generator start-up strategy. It first obtains the generator-starting sequence, then checks sequence feasibility by examining the satisfaction of various constraints. Authors in [17] proposed a load restoration model for transmission systems considering discrete load increments, cold load effect, reserve requirements, and other steady-state constraints. In this study, the LPAC is applied to the model restoration process and the security constraints are integrated to avoid infeasibility.

This study proposed an optimal repair crew deployment model to enhance transmission system resilience. The main contributions can be summarised as the following:

1. A proactive repair crew deployment model is proposed to minimise the expected load interruption. The model is formulated as a two-stage stochastic framework to make decisions considering post-disaster repair and restoration.
2. The proposed repair crew routing method considers the cooperation of repair crews to speed up the repair progress of critical components. Compared to most literatures limiting that each damaged component is repaired by only one of the crews, the proposed method can assign the repair work more efficiently and enable earlier restoration of critical load.
3. The whole restoration process including generator start-up, line energisation, and load restoration is modelled. Security constraints on line capacity, voltage magnitude, and reactive power are involved to avoid solution violations.
4. A scenario decomposition algorithm and preprocessing method to identify necessary components are introduced to cope with the computational challenges under emergency conditions.

The rest of this study is organised as follows. Section 2 describes the framework of the repair crew deployment model. Section 3 presents the mathematical formations. Section 4 provides the solution algorithm. Section 5 presents the case results, and Section 6 concludes the study.

2 | MODEL FRAMEWORK

The objective of the proposed model is to proactively allocate repair crews to candidate deployment locations to achieve emergency response after a hurricane strikes. After situational awareness of an upcoming hurricane, according to weather forecast, component fragility assessment, and vehicle travel-time estimation, damage scenarios are generated and the two-stage stochastic optimisation model is formulated. Figure 1 shows the model framework. In stage I, the repair crews are allocated to candidate locations to prepare for a hurricane. The deployment decisions are made to optimise the expected performance of second-stage repair and restoration under a number of scenarios.

To allocate the repair crews and their resources, some depots or buildings invulnerable to hurricanes and close to potentially damaged components are selected as candidate deployment locations. The geographic information system (GIS) can be integrated to evaluate the spatiotemporal impacts of disasters [18]. As demonstrated in the left part of Figure 2, a mesh plot is applied to approximately represent the component geographic locations. Each cell in the mesh plot is assumed to have homogeneous disaster intensity. The regional wind speed can be calculated according to the distance between the cell and hurricane eye [19] and the flood intensity can be estimated based on the regional rainfall [20, 21]. The component failure probability is acquired according to the disaster intensity and component fragility curve. The component's status is assigned by comparing each component's failure probability with a uniformly distributed random number within an interval (0, 1) [22].

A complete blackout is assumed for the system or sectionalised subsystem after the disaster strikes. The restoration and repair are co-optimised as shown in the right part of Figure 2. Regarding the fact that a time step in load restoration usually takes several minutes, while the one in vehicle travel and repair

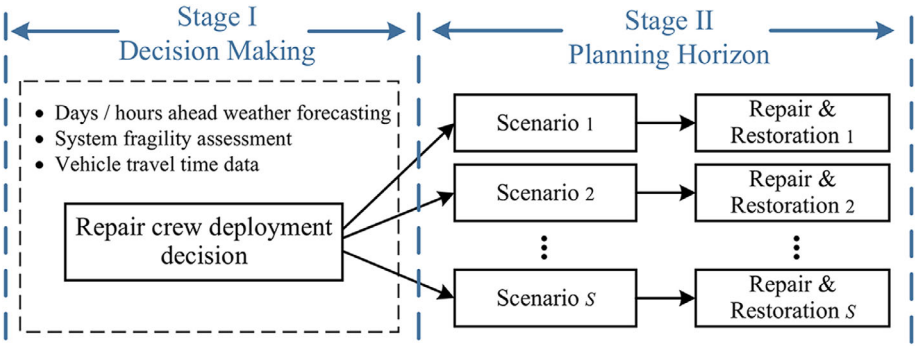

FIGURE 1 Framework of the two-stage stochastic model

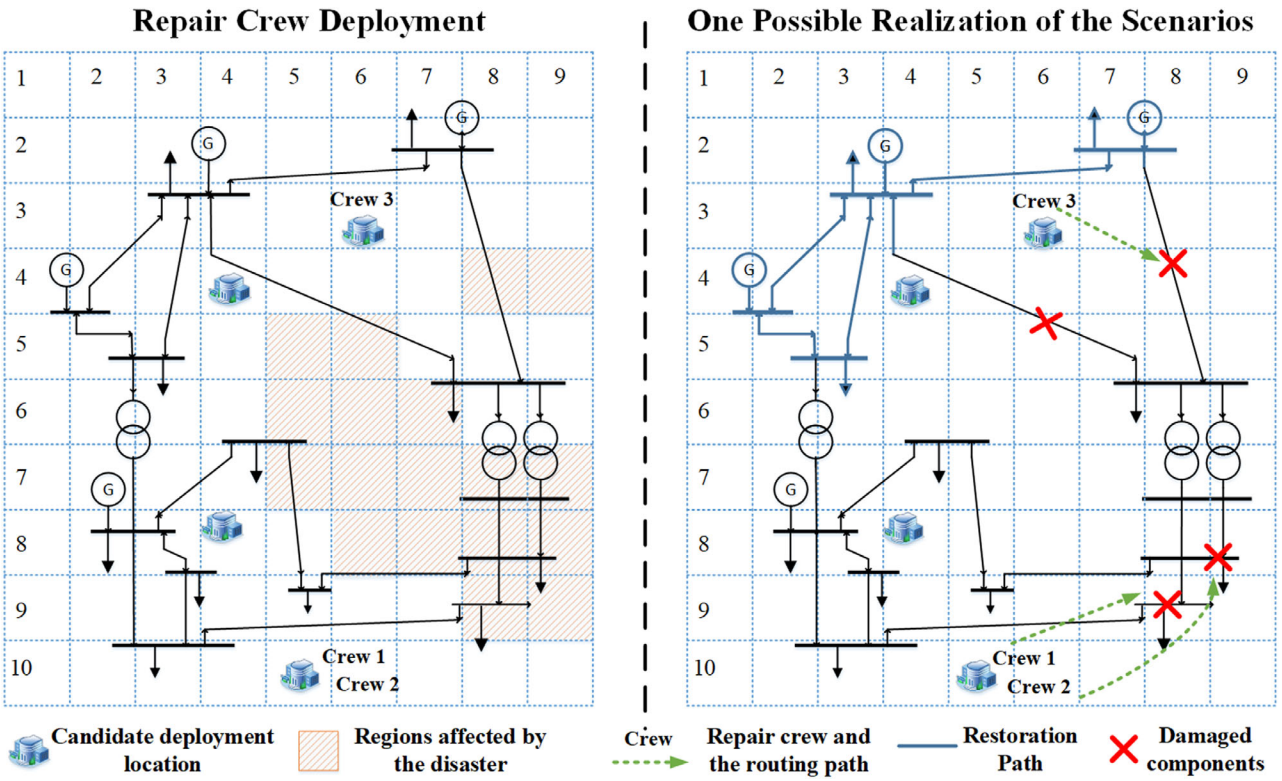

FIGURE 2 Process of crew deployment, repair, and restoration

takes hours, we use two coordinates with different time granularity to model the sequence of repair and restoration to reduce variables. Figure 3 shows an example of the time coordinates. To avoid confusion, we denote t and t' as the time-step index of repair and restoration, respectively.

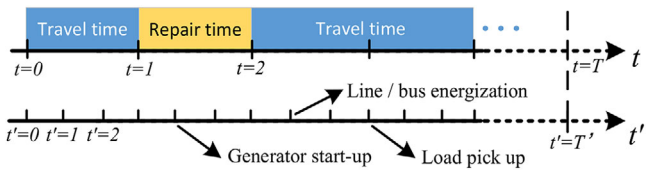

FIGURE 3 Time coordinates of repair and restoration

The required time and resources to fix a damaged component can be estimated during the damage assessment stage [9]. For deployment, we assume the required repair time and resources can be estimated through expert judgement based on components characters and disaster intensity.

3 | MATHEMATICAL FORMULATIONS

The objective function is to maximise the expected restored load and minimise the repair duration:

$$\max \sum_{s\in \mathbf{S}} \pi_s \left(\Delta t' \sum_{t'=1}^{T'} \sum_{j\in \mathbf{V}} w_j P_{j,t'}^{load,s} - \alpha \sum_{n\in \mathbf{N}^s} \sum_{t=1}^{T} t \cdot f_{n,t}^{s} \right) \quad (1)$$

where the first term indicates total restored loads considering their priorities. The second term denotes the total repair duration of damaged components with a weight α. The second term forces the crews proceeding their work to repair the rest of the damaged components after all loads are restored.

3.1 | Proactive deployment constraints

Prior to a natural disaster, the repair crews are deployed to candidate locations. The deployment constraint is to prevent each repair crew from being assigned to more than one candidate location, which is listed as follows:

$$\sum_{l \in CL} Dep_{c,l} \leq 1, \forall c \in Crew \tag{2}$$

3.2 | Repair dispatch constraints

3.2.1 | Repair crew routing

The repair crews routing formulations derive from the multi-depot vehicle routing problem (VRP) [23] repair crews set off from their deployed locations, visit all damaged components, and arrive at the return point *dp* after task completion.

$$\sum_{n \in \mathbf{N}} a^s_{l,c,n} \leq Dep_{c,l}, \quad \forall c \in Crew, l \in CL, s \tag{3}$$

$$\sum_{l} a^s_{l,c,n} + \sum_{m \in \mathbf{N}} x^s_{m,c,n} - \sum_{m \in \mathbf{N} \cup dp} x^s_{n,c,m} = 0, \quad \forall n \in \mathbf{N}^s, c \in Crew, s \tag{4}$$

$$\sum_{l \in Loc} a^s_{l,c,n} + \sum_{m \in \mathbf{N}} x^s_{m,c,n} \leq 1, \quad \forall n \in \mathbf{N}^s, c \in Crew, s \tag{5}$$

$$\sum_{n \in \mathbf{N}^s} x^s_{n,c,dp} = 1, \quad \forall c \in Crew, s \tag{6}$$

$$y^s_{n,c} = \sum_{m \in \mathbf{N}^s \cup dp} x^s_{n,c,m}, \quad \forall n \in \mathbf{N}^s, c \in Crew, s \tag{7}$$

$$\sum_{n \in \mathbf{N}^s} Res^{require}_n y^s_{n,c} \leq Res^{carry}_c, \quad \forall c \in Crew, s \tag{8}$$

Constraint (3) enforces one repair crew can leave from location *l* to damaged components only if it has been deployed to *l*. Constraint (4) makes sure that if one crew visits component *n*, the crew should also leave it. Constraint (5) prevents the crew from reaching the same component twice. After the task completion, all crews should go back to the return point *dp*, which is presented by Equation (6). In Equation (7), a binary variable $y^s_{n,c}$ is defined to determine whether crew *c* visits component *n*. Constraint (8) ensures the total resources required by components assigned to one crew should not exceed the crew's carrying capacity.

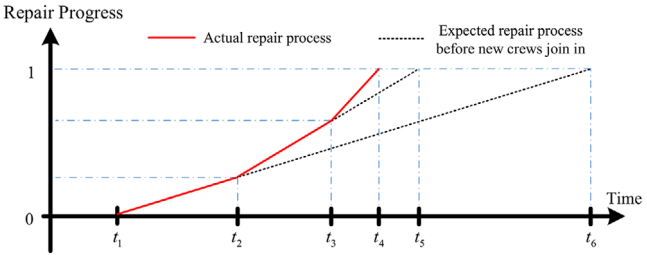

FIGURE 4 Accelerations of repair progress

3.2.2 | Arrival/departure time

The proposed repair routing method allows cooperation of repair crews to achieve rapid repair of critical components.

More crews assigned to one component can result in shorter repair time. We assume the repair progress of crews on a damaged component can be linearly superposed [14]. Figure 4 illustrates the repair progress of a specific component when new crews participating in the repair work successively. The required progress to complete repairing is normalised to 1. The first repair crew (crew 1) arrives and starts the repair at t_1 and the expected repair completion time is t_6. Then crew 2 joins in at t_2. The remaining repair work is accelerated and the expected completion time became t_5. After crew 3 joins in at t_3, the completion time is finally brought forward to t_4.

In addition, a saturation point is considered where more crews will not further accelerate the repair if the crew number exceeds the maximum requirement of the component.

On the basis of the above discussion, constraints on collaborative repair is formulated as follows:

$$\sum_{c \in Crew} t^{rep,s}_{n,c} \cdot \frac{1}{t^{require}_{n,c}} \geq 1, \quad \forall n \in \mathbf{N}^s, s \tag{9}$$

$$\sum_{t=1}^{T} t \cdot f^s_{n,t} \geq t^{arrive,s}_{n,c} + t^{rep,s}_{n,c}, \quad \forall n \in \mathbf{N}^s, c \in Crew, s \tag{10}$$

$$\sum_{t=1}^{T} f^s_{n,t} \leq 1, \quad \forall n \in \mathbf{N}^s, s \tag{11}$$

$$\sum_{c \in Crew} y^s_{n,c} \leq K_n, \quad \forall n \in \mathbf{N}^s, s \tag{12}$$

In constraint (9), $t^{require}_{n,c}$ is the required time for crew *c* to repair component *n* independently. By normalising the required progress to repair component *n* to 1, the repair speed of crew *c* can be represented as $\frac{1}{t^{require}_{n,c}}$. Constraint (9) means to have component *n* fixed, the summation of repair progress by participating crews should achieve 1. For example, in Figure 4, the repair progress contributed by crew 1, 2, and 3 is $(t_4 - t_1) \cdot \frac{1}{t^{require}_{n,1}}$, $(t_4 - t_2) \cdot \frac{1}{t^{require}_{n,2}}$ and $(t_4 - t_3) \cdot \frac{1}{t^{require}_{n,3}}$. The three items add up to 1 since the repair is completed at t_4. Constraint (10) ensures that

the repair of component n is completed only when the last crew finishes repairing n. Binary variable $f^s_{n,t}$ indicates whether component n is fixed at time t. Item $t \cdot f^s_{n,t}$ denotes the time that the component is brought back to normal status. The repair crews are not required to arrive at n at the same time. However, to have n fixed earlier, the arrival and repair time will be allocated optimally. Constraint (11) limits that the damaged component can be fixed only once. Constraint (12) indicates component n can be repaired by up to K_n crews at the same time. Parameter K_n can be determined according to the component characters.

The relationship between travel, arrival, and repair time is represented by Equations (13) to (15) [9].

$$0 \le t^{arrive,s}_{n,c} - \sum_{l\in CL} a^s_{l,c,n} t^{travel}_{l,c,n} \le (1 - \sum_{l\in CL} a^s_{l,c,n})M, \quad \forall n \in \mathbf{N}^s, c \in Crew, s \tag{13}$$

$$t^{arrive,s}_{n,c} + t^{rep,s}_{n,c} + t^{travel}_{n,c,m} - t^{arrive,s}_{m,c} \le (1 - x^s_{n,c,m})M, \quad \forall n \in \mathbf{N}^s, m \in \mathbf{N}^s \cup dp, c \in Crew, s \tag{14}$$

$$0 \le t^{rep,s}_{n,c} \le y^s_{n,c}M, \quad \forall n \in \mathbf{N}^s, c \in Crew, s \tag{15}$$

Constraint (13) determines the arrival time at the first component for each crew. If repair crew c departs from the deployed location l at the start and chooses damaged component n as the first component to repair, that is, $a^s_{l,c,n} = 1$, the arrival time at component n ($t^{arrive,s}_{n,c}$) should equal to the vehicle travel time it takes from the deployed location l to n ($t^{travel}_{l,c,n}$). Constraint (14) indicates the relationship between the arrival time at two damaged components. If crew c arrives at component n at time $t^{arrive,s}_{n,c}$ and travels the path from component n to m ($x^s_{n,c,m} = 1$), it takes crew c time $t^{rep,s}_{n,c}$ to repair component n and then time $t^{travel}_{n,c,m}$ to move from n to m, that is, the arrival time at component m ($t^{arrive,s}_{m,c}$) equals $t^{arrive,s}_{n,c} + t^{rep,s}_{n,c} + t^{travel}_{n,c,m}$. Constraint (15) ensures if crew c hasn't visited component n, the corresponding repair time is 0.

3.3 | Power system operational constraints

3.3.1 | Generator start-up

In power system restoration, generators can be divided into two groups according to their restart requirements: Black-start (BS) units that can start independently and non-black-start (NBS) units that require cranking power from outside to start.

Figure 5(a) shows a typical generator start-up curve during the restoration. The generator gets energised at time t_{start}. After receiving cranking power P^{CR}_g for T^{CR}_g time steps to initiate start up, it begins to ramp up within ramping rate K_g and parallel with the system. The output can be adjusted between $P^{\min}_g$ and $P^{\max}_g$ once it reaches the minimum generation $P^{\min}_g$.

As discussed in [24], the generator start-up curve can be decomposed as two parts: (1) An equivalent output curve shown in Figure 5(b), where the upper and lower limits of equivalent output are defined as $\overline{P}_g = P^{\max}_g + P^{CR}_g$ and $\underline{P}_g = P^{\min}_g + P^{CR}_g$,

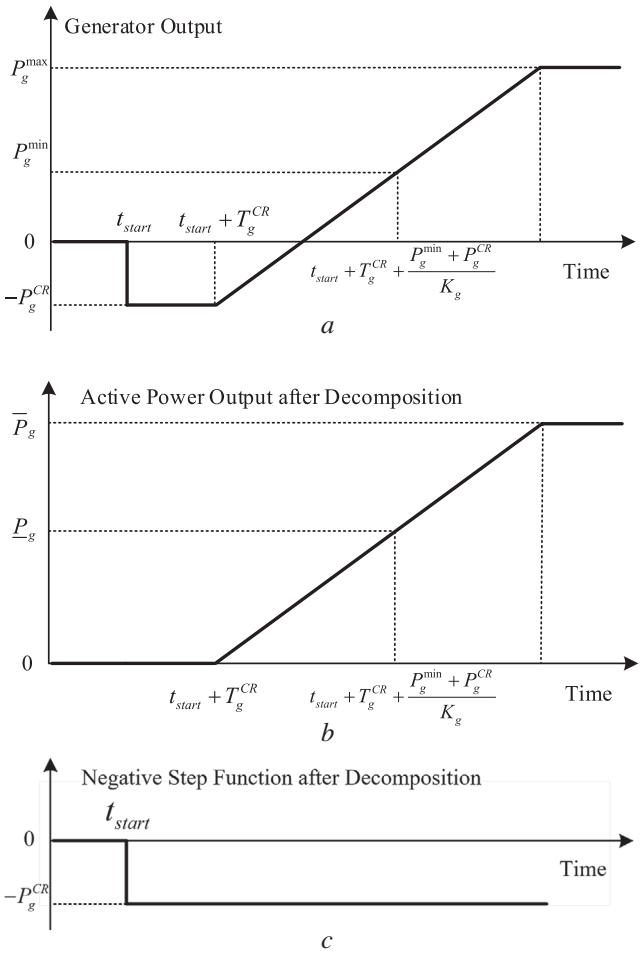

FIGURE 5 Typical generator start-up curve and its decomposition (a) generator start-up curve, (b) equivalent active power output after decomposition, and (c) negative step function of cranking power

and (2) a negative step function of the cranking power at the time of energisation, which can be seen in Figure 5(c). In doing so, the active power output curve is simplified as a three-segment output function superimposed by a negative step function. Note that for BS units, the cranking power P^{CR}_g is 0 [25]. However, the decomposition method and the following formulations are also suitable for BS units by setting P^{CR}_g as 0 and adjusting the negative step curve in Figure 5(c) to a function that always evaluates to 0.

On the basis of the decomposition, the generator start-up constraints can be formulated as Equations (16) to (21):

$$0 \le P^{G,s}_{g,\tau} \le \overline{P}_g En^{G,s}_{g,t'}, \forall \tau \in \{t', t'+1, \dots, t'+T^{CR}_g\}, \quad \forall t' = 0, 1, \dots, T - T^{CR}_g, \forall g \in G(j), \forall j \in \mathbf{V}, \forall s \tag{16}$$

$$P^{G,s}_{g,\tau} \ge \underline{P}_g En^{G,s}_{g,t'}, \forall \tau \ge t' + T^{CR}_g + \underline{P}_g / K_g, \quad \forall g \in G(j), \forall j \in \mathbf{V}, \forall t', s \tag{17}$$

$$\left| P^{G,s}_{g,t'} - P^{G,s}_{g,t'-1} \right| \le K_g \Delta t', \forall g \in G(j), \forall j \in \mathbf{V}, \forall t', s \tag{18}$$

$$En^{G,s}_{g,t'} \ge En^{G,s}_{g,t'-1}, \forall j \in \mathbf{V}, \forall t', s \tag{19}$$

Constraint (16) forces the active power outputs of both BS and NBS units to be 0 until the generators have been energised ($En^{G,s}_{g,t'} = 1$) for T^{CR}_g time steps [24]. Constraint (17) indicates that the minimum active power output limit should be satisfied after the generator ramps up to $\overline{P}_g$. The ramping up/down limits are guaranteed by Equation (18). Constraint (19) ensures the generator cannot shut down once it starts up.

3.3.2 | AC power flow and linear approximation

The active and reactive line flow formulations based on AC power flow are presented in Equation (21) [26].

$$\begin{cases} P^{L,s}_{ij,t'} = G_{ij}(U^{s2}_{i,t'} - U^s_{i,t'}U^s_{j,t'}\cos(\theta^s_{i,t'} - \theta^s_{j,t'})) \\ \quad - B_{ij}\left(U^s_{i,t'}U^s_{j,t'}\sin(\theta^s_{i,t'} - \theta^s_{j,t'})\right) \\ Q^{L,s}_{ij,t'} = -B_{ij}(U_{i,t'^{s2}} - U^s_{i,t'}U^s_{j,t'}\cos(\theta^s_{i,t'} - \theta^s_{j,t'})) \\ \quad - G_{ij}\left(U^s_{i,t'}U^s_{j,t'}\sin(\theta^s_{i,t'} - \theta^s_{j,t'})\right) \end{cases} \tag{20}$$

LPAC is applied to deal with the non-convex and nonlinear elements [27, 28]. Taking account of the line energisation status, constraint (20) is reformulated as Equations (21) and (22), where $r_{(i,j)}$ is the piecewise linear approximation of term $\cos(\theta^s_{i,t'} - \theta^s_{j,t'})$ on condition that $-\frac{\pi}{2} \le \theta^s_{i,t'} - \theta^s_{j,t'} \le \frac{\pi}{2}$

$$\begin{cases} P^{L,s}_{ij,t'} - (1 - En^{L,s}_{ij,t'})M \le G_{ij}(U^s_{i,t'} - U^s_{j,t'} - r_{(i,j)} + 1) \\ \quad - B_{ij}\left(\theta^s_{i,t'} - \theta^s_{j,t'}\right) \\ P^{L,s}_{ij,t'} + (1 - En^{L,s}_{ij,t'})M \ge G_{ij}(U^s_{i,t'} - U^s_{j,t'} - r_{(i,j)} + 1) \\ \quad - B_{ij}\left(\theta^s_{i,t'} - \theta^s_{j,t'}\right) \end{cases} \quad \forall (i,j) \in \mathbf{L}, \forall t', s \tag{21}$$

$$\begin{cases} Q^{L,s}_{ij,t'} - (1 - En^{L,s}_{ij,t'})M \le -B_{ij}(U^s_{i,t'} - U^s_{j,t'} - r_{(i,j)} + 1) \\ \quad - G_{ij}\left(\theta^s_{i,t'} - \theta^s_{j,t'}\right) \\ Q^{L,s}_{ij,t'} + (1 - En^{L,s}_{ij,t'})M \ge -B_{ij}(U^s_{i,t'} - U^s_{j,t'} - r_{(i,j)} + 1) \\ \quad - G_{ij}\left(\theta^s_{i,t'} - \theta^s_{j,t'}\right) \end{cases} \quad \forall (i,j) \in \mathbf{L}, \forall t', s \tag{22}$$

The power balance and load-shedding constraints are presented in Equations (24) to (26).

$$\sum_{\tau \in \delta(j)} P^{L,s}_{j\tau,t'} - \sum_{i \in \pi(j)} P^{L,s}_{ij,t'} = \sum_{g \in G_{NBS}(j)} \left(P^{G,s}_{g,t'} - P^{CR}_g En^{G,s}_{g,t'}\right) + \sum_{g \in G_{BS}(j)} P^{G,s}_{g,t'} - P^{load,s}_{j,t'}, \quad \forall j \in \mathbf{V}, \forall t', s \tag{23}$$

$$\varepsilon \cdot En^{V,s}_{j,t'} \le P^{load,s}_{j,t'} \le P^D_j \cdot En^{V,s}_{j,t'}, \quad \forall j \in \mathbf{V}, \forall t', s \tag{24}$$

$$P^{load,s}_{j,t'} \ge P^{load,s}_{j,t'-1}, \quad \forall j \in \mathbf{V}, \forall t', s \tag{25}$$

Equation (23) presents the power balance constraint. For a BS unit, the active power output is $P^{G,s}_{g,t'}$; whereas for an NBS unit, the cranking power is provided by either nearby BS generators or line flows, therefore a negative term $-P^{CR}_g$ should be reckoned in to calculate the net active power output if the unit is energised ($En^{G,s}_{g,t'} = 1$). Constraint (24) states that the loads can be picked up only if the bus is energised. We assume the load can be picked up continuously since the amount of restored load is usually comprised of small discrete load increments [24]. A very small constant ε is introduced to help ensure that the energised bus is always connected to power sources through an energisation path. Constraint (25) makes sure that once a load is picked up, it should not be curtailed during the following time steps. The combination of Equations (24) and (25) prevents the energised bus from being de-energised.

3.3.3 | Security constraints

The branch flow and voltage should be within their feasible ranges.

$$\sqrt{\left(P^{L,s}_{ij,t'}\right)^2 + \left(Q^{L,s}_{ij,t'}\right)^2} \le S^{\max}_{ij} En^{L,s}_{ij,t'}, \quad \forall (i,j) \in \mathbf{L}, \forall t', s \tag{26}$$

$$U_{\min} \le U^s_{j,t'} \le U_{\max}, \quad \forall j \in \mathbf{V}, \forall t', s \tag{27}$$

The quadratic security in constraint (26) forms a circular feasible region in P-Q coordinate, which can be approximated to several square regions and linearised as discussed in [29].

The reactive power in the system or sectionalised subsystem should be balanced [25], which can be achieved by controlling generators and load with lagging power factors and line energisation status:

$$\sum_{\kappa \in \delta(j)} Q^{L,s}_{j\kappa,t'} - \sum_{i \in \pi(j)} Q^{L,s}_{ij,t'} + \sum_{g \in G(j),} \underline{Q}_g En^{G,s}_{g,\max(0,t'-T^{CR}_g)} + \sum_{i \in \pi(j) \cup \delta(j)} \frac{1}{2} B_{ij} U^2 En^{L,s}_{ij,t'} - P^{load,s}_{j,t'} \tan\left(\theta_j\right) \le 0, \quad \forall j \in \mathbf{V}, \forall t', s \tag{28}$$

By aggregating this constraint of nodes in each energised section, it can be guaranteed that the capability of generators and load to absorb reactive power is larger than the reactive power generated by the high capacitance of lines [24]. The bus voltage U and voltage phase θ_j here are assumed to be 1 and a constant for linearisation.

3.4 | Relations of component status and energisation

Fault statuses of transmission lines and substations are considered for transmission systems that suffered from both hurricanes and hurricane-induced floods:

$$Fix_{i,t}^{V,s} = \sum_{t=1}^{T} f_{i,t}^{s}, \quad \forall i \in DB^{s}, \forall t, s \tag{29}$$

$$Fix_{ij,t}^{L,s} = \sum_{t=1}^{T} f_{\kappa,t}^{s}, \quad \forall (i,j) \in DL^{s}, \forall t, s \tag{30}$$

Constraints (29) and (30) determine the repair status of the damaged components. The damaged component will be available ($Fix_{i,t}^{V,s} = 1, Fix_{ij,t}^{L,s} = 1$) after it is repaired. Subscript κ in Equation (30) denotes the component index of the line (i,j).

The long transmission line can be split into several sections for accurate dispatch as mentioned in [30]. The proposed model can be expanded for this purpose by introducing series variables $f_{\kappa(1),t}^{s}, f_{\kappa(2),t}^{s}, \dots, f_{\kappa(nl),t}^{s}$ as the repair indicators of nl sections of the transmission line κ. Then the status relations of the line and its sections can be represented by reformulating constraint (30) as $Fix_{ij,t}^{L,s} \le \sum_{t=1}^{T} f_{\kappa(1),t}^{s}, Fix_{ij,t}^{L,s} \le \sum_{t=1}^{T} f_{\kappa(2),t}^{s}, \dots, Fix_{ij,t}^{L,s} \le \sum_{t=1}^{T} f_{\kappa(nl),t}^{s}$. Note that the exact fault location for a transmission line is usually identified after repair crews arrive. So we take a line as one component and use the middle section to represent its location.

The damaged component can participate in the restoration once the repair is completed. The repair status variables at time step t and energisation variables at t' are coupled as follows:

$$\begin{cases} En_{g,t'}^{G,s} \le En_{j,t'}^{V,s} \le Fix_{j,t}^{V,s}, \quad \forall g \in G(j), \forall j \in \mathbf{V}, \forall s \\ En_{ij,t'}^{L,s} \le Fix_{ij,t}^{L,s}, \quad \forall (i,j) \in \mathbf{L}, \forall s \\ \forall t' \in \{\lambda(t-1)+1, \lambda(t-1)+2, \dots, \lambda t\}, \forall t \end{cases} \tag{31}$$

where λ is the scale ratio of one step in time coordinates t and t'. The upper formula means bus j can be energised only if it is repaired or not damaged. Moreover, if a generator connected to bus j is energised, then j should be energised. Similarly, the lower formula restricts the energisation of transmission lines.

The restoration sequence is modelled by the following constraints:

$$En_{ij,t'}^{L,s} \le En_{i,t'-1}^{V,s} + En_{j,t'-1}^{V,s}, \quad \forall (i,j) \in \mathbf{L}, \forall t', s \tag{32}$$

$$En_{ij,t'}^{L,s} \le En_{i,t'}^{V,s}, En_{ij,t'}^{L,s} \le En_{j,t'}^{V,s}, \quad \forall (i,j) \in \mathbf{L}, \forall t', s \tag{33}$$

Constraint (32) ensures that a line can be energised only when one of the buses connected to it gets energised in the previous time step. In addition, if a line is energised, the buses at both ends should also get energised, which is represented by Equation (33).

ALGORITHM 1 PH algorithm

1: **Initialisation**: Set $k = 0$, $\omega_s^{(k)} = 0$, gap, ρ. For all $s \in \mathbf{S}$, compute: $h_s^0 = \arg\min_{h,\zeta_s} \{p \cdot h + q_s \cdot \zeta_s : (h, \zeta_s) \in K_s\}$.
2: **Iteration update**: $k = k + 1$
3: **Aggregation**: $\bar{h}^{(k)} = \sum_{s \in \mathbf{S}} \pi_s \cdot h_s^{(k)}$
4: **Multiplier update**: For all $s \in \mathbf{S}$, $\omega_s^{(k)} = \omega_s^{(k-1)} + \rho \left(h_s^{(k)} - \bar{h}^{(k)} \right)$
5: **Decomposition**: For all $s \in \mathbf{S}$, compute: $h_s^{(k)} = \arg\min_{h,\zeta_s} \left\{ p \cdot h + q_s \cdot \zeta_s + \omega_s^{(k)} \cdot h + \frac{\rho}{2} \left\| h - \bar{h}^{(k-1)} \right\|^2 : (h, \zeta_s) \in K_s \right\}$
6: **Termination**: If $\sum_{s \in \mathbf{S}} \pi_s \left\| h_s^{(k)} - \bar{h}^{(k)} \right\| < gap$, terminate. Otherwise go to step 2.

3.5 | The final repair crew deployment model

The final form of the proposed model is as follows:

Objective: Equation (1)

Subject to Equations (2) to (19), (21) to (33).

which is an extensive form (EF) of the two-stage stochastic optimisation model and can be transformed into a mixed-integer linear programming problem. The original problem can be decomposed into several scenario-based sub-problems to reduce computational complexity.

4 | MODEL SOLUTION

4.1 | Progressive hedging (PH) algorithm

We apply the PH algorithm [31] to solve the two-stage stochastic mixed-integer problem. For the EF problem with $|\mathbf{S}|$scenarios, PH algorithm can decompose it into $|\mathbf{S}|$ subproblems by relaxing the non-anticipativity constraints and penalising the disagreement of the first-stage decision variables iteratively.

To simplify the notation, we denote the first-stage decision variables $Dep_{G,l}$ as vector$h$, other scenario-based variables as vector ζ_s. The implementation of PH algorithm is sketched in algorithm 1. In step 1, the iteration count$k$, multipliers $\omega_s^{(k)}$, convergence tolerance gap, and penalty coefficient ρ are initialised. The relaxed scenario subproblem is solved to obtain the first-stage decision variables h_s^0 for individual scenario s, where p and q_s denote the cost coefficients of the first- and second-stage variables. The iteration starts from step 2. In step 3, the solutions are aggregated based on scenarios probability to obtain the expected value $\bar{h}^{(k)}$. The multipliers $\omega_s^{(k)}$are updated in step 4. In step 5, the subproblem augmented with a linear term and a squared two-norm term penalising deviation of $h_s^{(k)}$ from $\bar{h}^{(k-1)}$ is re-solved, where $h_s^{(k)}$ is the first-stage decision variables for scenario s obtained in the kth iteration. The procedure will repeat until the non-anticipativity constraints are satisfied within the convergence tolerance.

PH algorithm may encounter cycling behaviour (some decision variables oscillate along with iteration) in the presence of

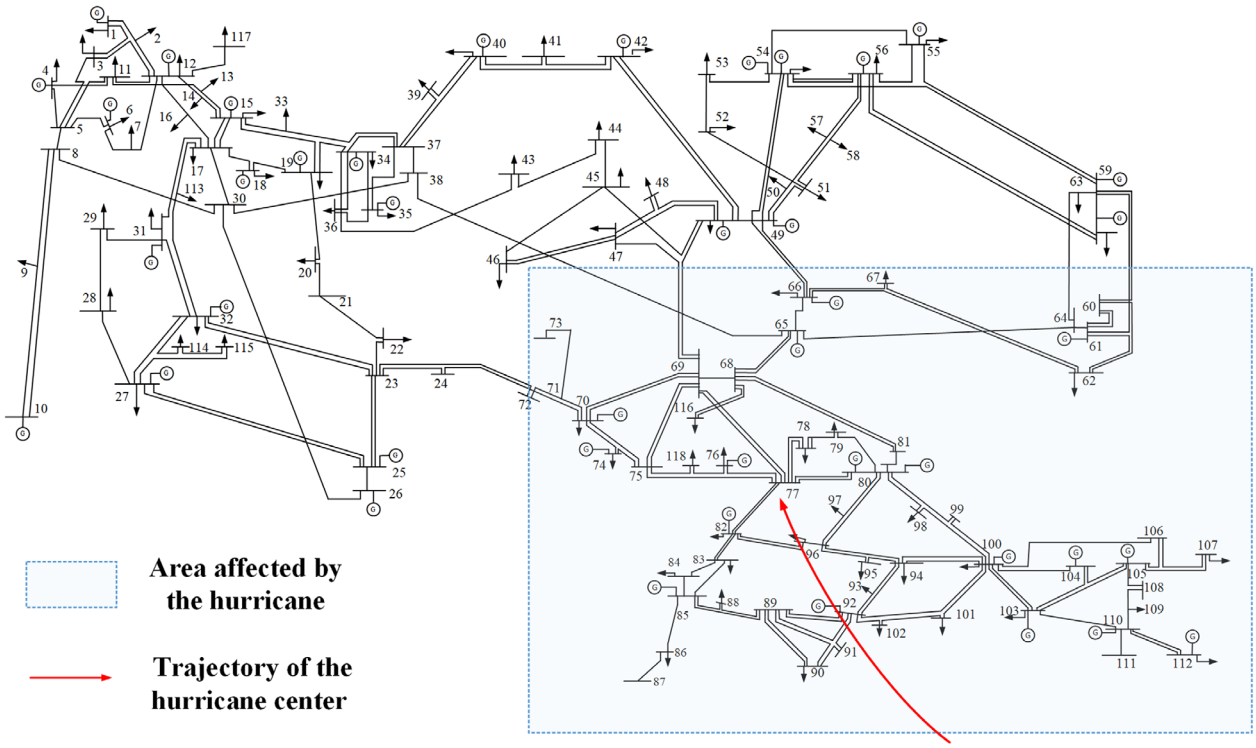

FIGURE 6 Geographical layout of the transmission system

integer variables despite the well-chosen ρ values [31], which prevents the algorithm convergence. We use the method in [32] to detect cycles, that is, using a simple hashing scheme and focusing on repeated occurrences of the multipliers vectors. To break cycles, the following procedure is adopted: Every time the cycling behaviour is detected, one oscillated variable is slammed to its maximum or minimum value and is constrained as a constant value in the following iterations. The procedure can ensure convergence with a minimal impact on solution quality since only a few variables will encounter oscillation.

4.2 | Identify necessary components

The computational burden increases with the number of damaged components. We proposed a preprocessing method to identify a set of necessary components to be repaired for each scenario in order to further reduce the computation time. We denote the set of necessary components as $\mathbf{N}^s_{sub}$ which is a subset of $\mathbf{N}^s$. To avoid sacrificing the optimality, the necessary components are selected following the criteria that if the components in $\mathbf{N}^s_{sub}$ are brought into normal status, not only all load can be picked up, but the time to pick up each load will not be delayed compared to repairing all damaged components in $\mathbf{N}^s$. The method to identify necessary components for scenario s is formulated as follows:

$$\max \Delta t' \sum_{t'=1}^{T'} \sum_{j \in \mathbf{V}} w_j P^{load,s}_{j,t'} - \gamma \left(\sum_{i \in DB^s} Fix^{V,s}_{i,T} + \sum_{(i,j) \in DL^s} Fix^{L,s}_{ij,T} \right) \tag{34}$$

Subject to Equations (16) to (19), (21) to (28), (31) to (33)

$$Fix^{V,s}_{i,t} \geq Fix^{V,s}_{i,t-1}, \quad \forall i \in DB^s, \forall t \tag{35}$$

$$Fix^{L,s}_{ij,t} \geq Fix^{L,s}_{ij,t-1}, \quad \forall (i,j) \in DL^s, \forall t \tag{36}$$

where γ is a small weight value. The objective function is to maximise the restored load during the whole process with a possible minimum number of damaged components which are available at time step T. Constraints (35) and (36) state that if a damaged bus or line is selected to be repaired, it should be kept available until time step T. Comparing to repairing all components, repairing the selected ones can achieve the same restoration performance. So we can just assign the necessary components to repair crews and keep other damaged components de-energised in the whole process to improve the computation efficiency.

5 | CASE STUDY

5.1 | Test system introduction

The IEEE 118-bus system [33] is applied to test the proposed model. The system's geographical layout is assumed to be the way as shown in Figure 6 [18]. The area may be affected by the upcoming hurricane as shown in the dotted frame. Assume there are 17 components with failure risk which are marked with red triangles in Figure 7. The failure probability, repair time, and repair resources of the components are listed in Table 1. The

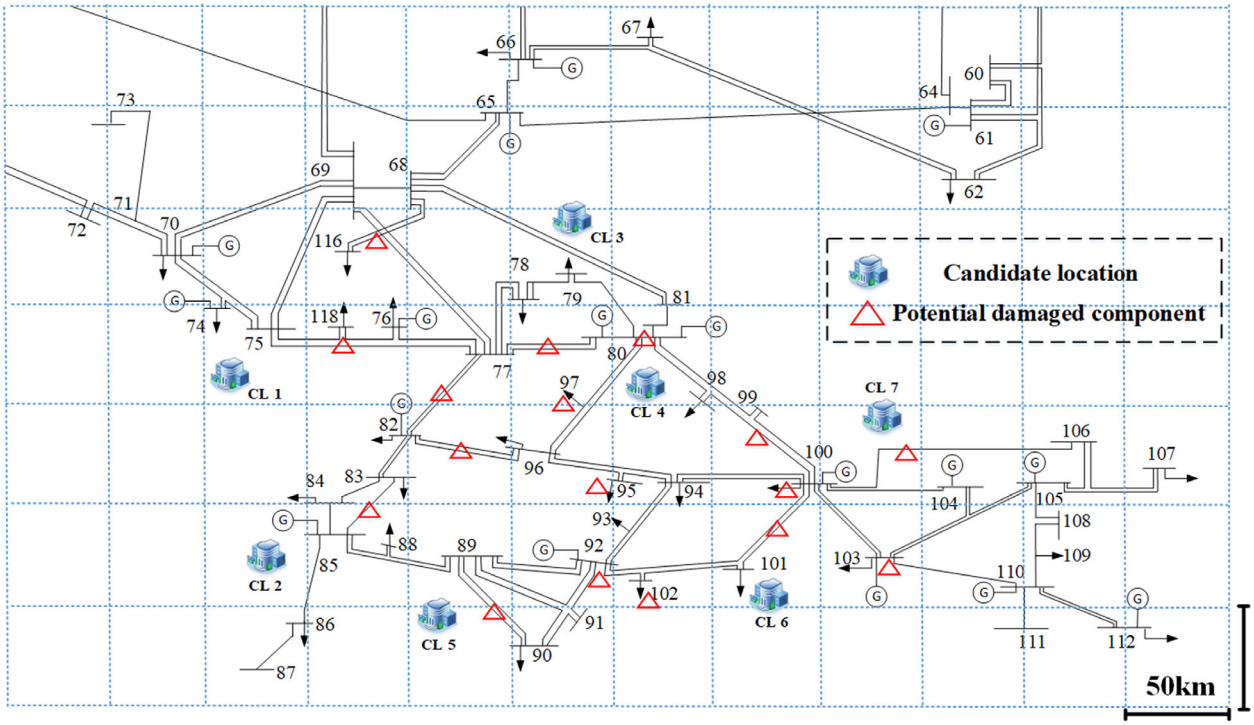

FIGURE 7 The region affected by the hurricane

TABLE 1 Information of the potential damaged components

Component		Component index	Failure probability	Repair time (h) for single crew	Required resources
Bus	B92	N1	0.30	3	4
	B100	N2	0.20	2	4
	B118	N3	0.40	2	3
	B95	N4	0.15	5	3
	B102	N5	0.20	2	4
	B80	N6	0.35	2	3
	B103	N7	0.10	3	3
	B97	N8	0.30	2	3
Line	L98–100	N9	0.25	3	3
	L82–96	N10	0.20	2	5
	L77–80	N11	0.35	2	4
	L89–90	N12	0.15	3	5
	L100–101	N13	0.30	2	5
	L68–116	N14	0.40	3	5
	L83–85	N15	0.25	2	5
	L77–82	N16	0.20	3	4
	L100–106	N17	0.20	2	4

whole system is assumed to undergo a blackout after a hurricane passes. A time step of repair and restoration is set as 1 h and 15 min, respectively. The optimisation time horizon is set as $T = 10$ h and $T' = 40$.

Assume there are seven candidate locations that are safe and proper for crew deployment, which are located near bus 75, bus 85, line 68–81, bus 80, bus 89, bus 101, and line 100–104, respectively, as shown in Figure 7. Five repair crews are on standby for deployment and the travel speed of each crew is 50 km/h. The maximum number of teams that can work simultaneously at a substation or line is set as 2. The maximum repair resource each crew can carry is 10 units. The generator at bus 59 is assigned as a BS unit. The cranking power, cranking time, and ramping limit of generators are referred from [34]. There are some buses with zero active load demand, whose energisation will be prevented by constraint (25). For these buses, a very small value of load demand is set to enable the energisation. The problems are modelled in MATLAB and solved by Gurobi-8.1.0 on a PC with Intel Core i7-6700 3.40 GHz CPU and 8 GB RAM.

TABLE 2 Optimal and random crew deployment result

Repair crew	Crew 1	Crew 2	Crew 3	Crew 4	Crew 5
Optimal location	CL4	CL1	CL4	CL6	CL1
Random location	CL2	CL3	CL3	CL6	CL7

5.2 | Importance of proactive repair crew deployment

In the case without proactive deployment, the repair crews will depart from the utility companies directly. We use random deployment to imitate the case without deployment, that is, randomly allocate crews to candidate locations and use the allocated locations to represent the utility companies. The performance of optimal deployment and random deployment are compared to show the effect of proactive deployment.

The optimal deployment decision under 20 scenarios and random deployment results are shown in Table 2. Optimal and

TABLE 3 Average restored load and repair time

	Case I	Case II
Average restored load	34,605 MWh	34227 MWh
Average repair completion time	7.50 h	8.35 h

TABLE 4 Average arrive time on first component (h)

	Crew 1	Crew 2	Crew 3	Crew 4	Crew 5
Case I	1.45	1.70	1.40	1.90	1.70
Case II	2.30	2.65	2.75	2.60	2.65

random deployment cases are denoted as case I and case II. The second-stage repair and restoration problem is solved under 50 randomly generated scenarios. The average restored load during the optimisation horizon and average time to complete all repair work of the two cases are listed in Table 3.

As indicated in Table 3, the number of restored load increases by hundreds of megawatt-hours, and the repair time goes down by 9.2% through optimal deployment. Table 4 shows the average arrival time to the first damaged component of each crew. The result indicates that it takes much longer for crews randomly deployed to reach damaged components.

TABLE 5 Component repair and load restoration of two cases

Time	$t' = 9, t = 3$ h		$t' = 17, t = 5$ h		$t' = 25, t = 7$ h	
Case	Case I	Case II	Case I	Case II	Case I	Case II
Repaired component	N3	–	N3, N8, N1, N16	N17, N3, N8	N3, N8, N1, N16, N4	N17, N3, N8, N1
Restored load (MW)	2750	2649	4201	4136	4242	4200
Load restoration increment (MW)	91		65		42	

Next, we select a representative scenario with damaged components B92, B118, B95, B97, L98–100, L89 and L90, L77–82, and L100–106 (labelled by N1, N3, N4, N8, N9, N12, N16, and N17) to further show the effect of optimal crew deployment. Through preprocessing, N1, N3, N4, N8, N16, and N17 are identified as necessary components. The components which have been repaired and the restored load of two cases in three time steps are shown in Table 5.

In case I, the repair progresses faster and a notable improvement in load restoration can be observed. Through proactive deployment, the response capability is enhanced and the post-disaster load curtailment is effectively mitigated.

5.3 | Effect of considering repair crews cooperation

To test the effect of repair crew cooperation, the deployment models with and without allowing collaborative repair are solved under 20 scenarios. In both cases, the second-stage variables in the last iteration are studied. The average restored loads across scenarios of both cases during $t' = 9\sim24$ ($t = 3\sim6$ h) are shown in Figure 8.

Through collaborative repair, more load can be picked up especially in the first several time steps due to the rapid repair of critical components.

For a detailed demonstration, a scenario with damaged components B95, B102, B103, L82–96, L77–80, L68–116, and L100–106 (labelled by N4/N5/N7/N10/N11/N14/N17) is chosen to illustrate the repair process. Among the components N4, N5, N7, N11, N14, and N17 are identified as necessary components. The crew routing results of the two cases are shown in Tables 6 and 7.

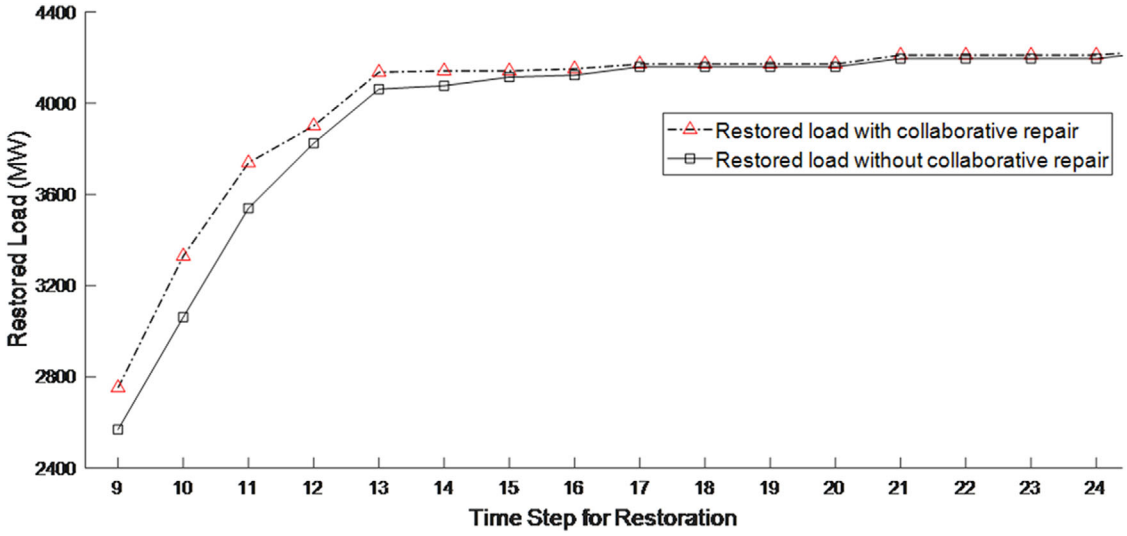

FIGURE 8 Average restored load of the two cases

TABLE 6 Crew routing with collaborative repair

Time step (h)	1	2	3	4	5	6	7	8	9	10
Crew 1	→	N4	N4	N4	→	→	N11	*dp*		
Crew 2	→	→	N14	N14	*dp*					
Crew 3	→	N4	N4	→	→	N5	N5	*dp*		
Crew 4	→	N7	N7	N7	→	→	N17	N17	*dp*	
Crew 5	→	→	N14	→	→	→	N11	*dp*		

TABLE 7 Crew routing without collaborative repair

Time step (h)	1	2	3	4	5	6	7	8	9	10
Crew 1	→	N4	N4	N4	N4	N4	*dp*			
Crew 2	→	→	→	N11	N11	*dp*				
Crew 3	→	→	→	N5	N5	*dp*				
Crew 4	→	N7	N7	N7	→	→	N17	N17	*dp*	
Crew 5	→	→	N14	N14	N14	*dp*				

Among the damaged components, the repair of N4, N7, and N14 can pick up loads over 20 MW. They are regarded as critical components of this scenario and marked with coloured rectangles in Tables 6 and 7. Without collaborative repair, N4 and N14 become operable at $t = 7$ h and $t = 6$ h. The relevant time is brought forward to $t = 5$ h through crew cooperation. It proves the advantage of the proposed routing method, through which the repair capacity is utilised more efficiently.

The optimal restoration and repair process of the affected area at $t' = 9$, $t = 3$ h is shown in Figure 9. It can be seen that the restoration of load at B116 is put off due to the damage status of L68–116. However, the cooperation of repair crew 2 and 5 will accelerate the repair progress to restore load 116 earlier.

At $t' = 16$, all load in the non-fault area is picked up. Restoration of the whole system is completed at $t' = 17$ and the repair work finishes in 8 h.

5.4 | Computational efficiency

Table 8 compares the computational efficiency of using PH algorithm, identifying necessary components (INC) and directly solving EF problem. The penalty factor ρ of PH algorithm is set as 10,000 and the solver MIPGap for both EF and PH is set as 0.5%. The maximum solution time of INC preprocessing for each scenario is 151 s.

As the scenario number increases, the computational burden of EF problem raises dramatically. PH algorithm can effectively manage this issue since it decomposes the original problem into scenario-based subproblems. The results also show the importance of INC in reducing calculation time. The computation time is acceptable since wind-related weather disasters are usually predicated days ahead, and PH algorithm is easily parallelised for efficient calculation.

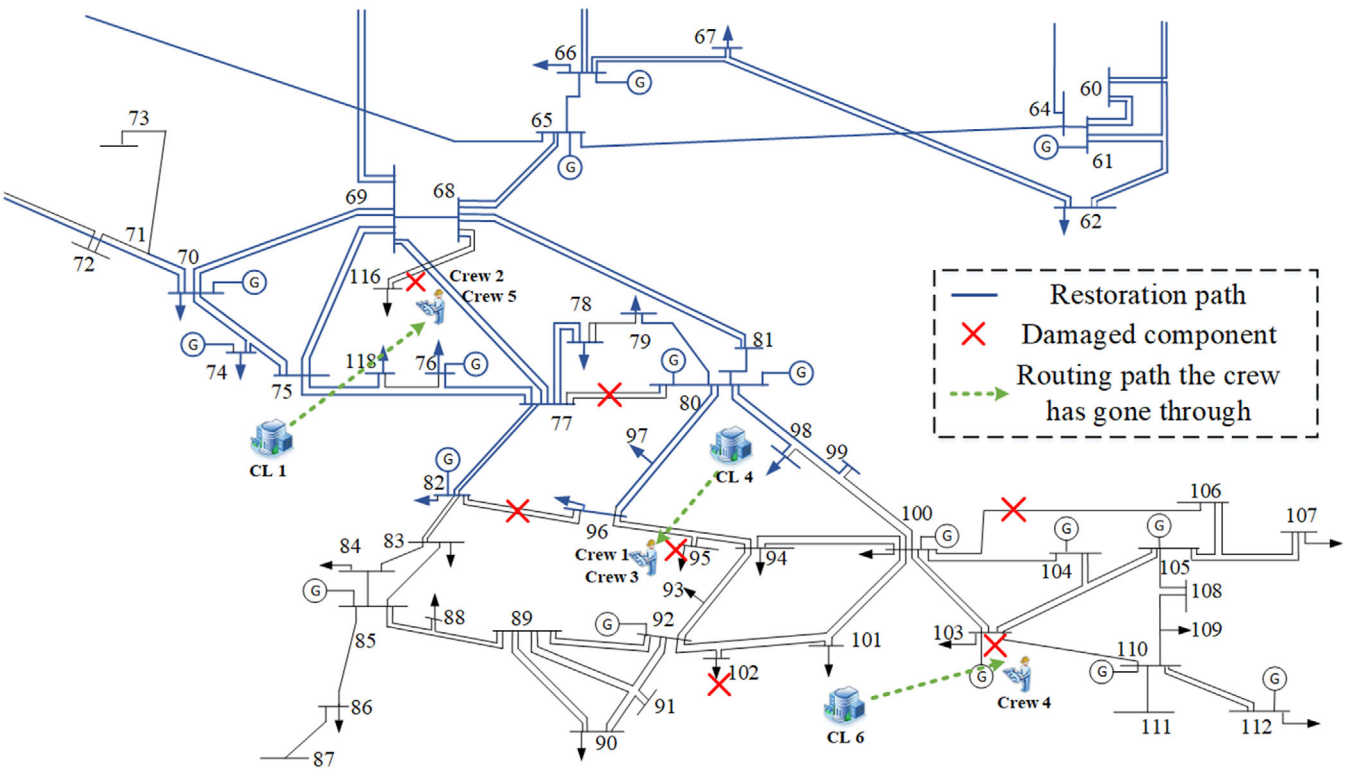

FIGURE 9 Restoration and repair process at $t' = 9$, $t = 3$ h

TABLE 8 Computation time of progressive hedging (PH) algorithm and extensive form (EF)

Number of scenarios	Solution method	Run time (h) with identifying necessary components (INC)	Run time (h) without INC
5	PH algorithm	3.9	6.7
	EF	**1.1**	3.3
10	PH algorithm	**9.7**	19.2
	EF	10.5	>30
20	PH algorithm	**26.2**	>30
	EF	>30	>30

6 | CONCLUSIONS

This study proposed an optimal repair crew deployment model to improve the responsibility and resilience of transmission systems against hurricanes. A repair crew routing method considering team cooperation is designed and the transmission system restoration process is integrated. The computational complexity of the two-stage stochastic model is tackled by PH decomposition algorithm. A preprocessing method to identify necessary components is proposed to further reduce the computation time. Case studies validate the effect of the proposed model.

Some issues are to be addressed in further work. For large-scale networks, the paralleled sectionalised restoration method will enhance the restoration efficiency. Moreover, combining the restoration with network reconfiguration techniques such as bus splitting is also a meaningful topic.

Nomenclature

Indices and sets

$\mathbf{V}$	set of buses
$\mathbf{L}$	set of transmission lines
$\mathbf{G}$	set of generators
$\mathbf{N}^s$	set of damaged components under scenario s
$\pi(j)/\delta(j)$	set of parent/child buses of bus j
t, t'	indexes of the time step for repair and restoration
$G(j)/G_{BS}(j)/G_{NBS}(j)$	set of generators/black-start units/non-black-start units connected to bus j
$DB^s/DL^s/DG^s$	set of damaged buses/transmission lines/generators under scenario s
c, $Crew$	index and set of repair crews
dp	index for return point after repair completion
l, CL	index and set of candidate locations for repair crew deployment
n, m	index of components
s, $\mathbf{S}$	index and set of scenarios

Parameters

π_s	probability factor of scenario s
w_j	priority weight of load at bus j
$\underline{Q}_g$	minimum reactive power output of g
$S_{ij}^{\max}$	apparent power capacity of the line (i, j)
$Res_n^{require}$	required resources to fix component n
Res_c^{carry}	maximum repair resource crew c can carry
$t_{n,c,m}^{travel}$	vehicle travel time for crew c to move from component n to m
$t_{l,c,m}^{travel}$	vehicle travel time for crew c to move from deployed location l to component m
$t_{n,c}^{require}$	required repair time of crew c to fix damaged component n
K_n	maximum number of repair crews that can work simultaneously at component n
$\Delta t'$	duration of a time step for restoration
$\overline{P}_g/\underline{P}_g$	maximum/minimum power output of generator g after the decomposition
T, T'	duration of optimisation time horizon for repair and restoration
G_{ij}/B_{ij}	conductance/susceptance of line (i, j)
$U_{\max}/U_{\min}$	maximum/minimum voltage magnitude
$P_g^{G,\max}/P_g^{G,\min}$	maximum/minimum power output of generator g before the decomposition
P_g^{CR}/T_g^{CR}	cranking power/time for non-black-start units to start up
M	a sufficiently large number

Variables

$Dep_{c,l}$	binary variable equals 1 if repair crew c is deployed to location l
$a_{l,c,n}^s$	binary variable equals 1 if crew c moves from location l to component n in scenario s
$x_{m,c,n}^s$	binary variable equals 1 if crew c moves from component m to n under scenario s
$y_{n,c}^s$	binary variable equals 1 if component n is repaired by crew c under scenario s
$f_{n,t}^s$	binary variable equals 1 if component n is repaired at time step t under scenario s
$P_{g,t'}^{G,s}$	active power output (after the decomposition) of generator g at time step t' under scenario s
P_j^D	active power load demand at bus j
$P_{j,t'}^{load,s}$	restored load at bus j at time step t' under scenario s
$t_{n,c}^{arrive,s}/t_{n,c}^{rep,s}$	arrival/repair time of crew c at component n
$Fix_{j,t}^{V,s}/Fix_{i,j,t}^{L,s}$	binary variable which equals 1 if bus j/line (i, j) is available at time step t under scenario s
$U_{j,t'}^s/\theta_{j,t'}^s$	voltage magnitude/voltage phase of node j at time step t' under s

$P^{L,s}_{i,j,t'}/Q^{L,s}_{i,j,t'}$ active/reactive power flow from node i to j at time step t' under scenario s

$En^{V,s}_{j,t'}/En^{L,s}_{i,j,t'}/En^{G,s}_{g,t'}$ binary variable which equals 1 if bus j/line (i, j)/generator g is energised at time step t' under scenario s

ACKNOWLEDGEMENTS

This work was supported by Science and Technology Project of State Grid (5202011600UG), China.

ORCID

Yiheng Bian https://orcid.org/0000-0002-7377-3878

REFERENCES

1. Bostrom, A., et al.: Eyeing the storm: How residents of coastal Florida see hurricane forecasts and warnings. Int. J. Disaster Risk Reduct 30, 105–119 (2018)
2. Hussain, A., et al.: Microgrids as a resilience resource and strategies used by microgrids for enhancing resilience. Appl. Energy 240, 56–72 (2019)
3. Ingargiola, J., et al.: Mitigation assessment team report: Hurricane Sandy in New Jersey and New York, building performance observations, recommendations, and technical guidance. Federal Emergency Management Agency (FEMA). https://doi.org/10.7282/T3J67F96)' (2013)
4. Wang, Y., et al.: Research on resilience of power systems under natural disasters—a review. IEEE Trans. Power Syst. 31(2), 1604–1613 (2016)
5. Zhou, Q., Chen, S.: Enhancing resilience of interdependent traffic-electric power system. Reliab. Eng. Syst. Saf. 191, 1–18 (2019)
6. Gholami, A., et al.: Proactive management of microgrids for resiliency enhancement: An adaptive robust approach. IEEE Trans. Sustainable Energy 10(1), 470–480 (2019)
7. Gao, H., et al.: Resilience-oriented pre-hurricane resource allocation in distribution systems considering electric buses. Proc. IEEE 105(7), 1214–1233 (2017)
8. Wang, C., et al.: Resilience enhancement with sequentially proactive operation strategies. IEEE Trans. Power Syst. 32(4), 2847–2857 (2017)
9. Arif, A., et al.: Power distribution system outage management with Co-optimization of repairs, reconfiguration, and DG dispatch. IEEE Trans. Smart Grid 9(5), 4109–4118 (2018)
10. Lei, S., et al.: Resilient disaster recovery logistics of distribution systems: Co-optimize service restoration with repair crew and mobile power source dispatch. IEEE Trans. Smart Grid 10(6), 6187–6202 (2019)
11. Arif, A., et al.: Repair and resource scheduling in unbalanced distribution systems using neighborhood search. IEEE Trans. Smart Grid 11(1), 673–685 (2020)
12. Lin, Y., et al.: A combined repair crew dispatch problem for resilient electric and natural gas system considering reconfiguration and DG islanding. IEEE Trans. Power Syst. 34(4), 2755–2767 (2019)
13. Coffrin, C., Van Hentenryck, P.: Transmission system restoration: Co-optimization of repairs, load pickups, and generation dispatch. In: 2014 Power Systems Computation Conference, Wroclaw, Poland, pp. 1–8 (2014)
14. Morshedlou, N., et al.: Work crew routing problem for infrastructure network restoration. Transp. Res. Part B Methodol. 118, 66–89 (2018)
15. Sun, L., et al.: Optimal skeleton-network restoration considering generator start-Up sequence and load pickup. IEEE Trans. Smart Grid 10(3), 3174–3185 (2019)
16. Sun, W., et al.: Optimal generator start-up strategy for bulk power system restoration. IEEE Trans. Power Syst. 26(3), 1357–1366 (2011)
17. Qin, Z., et al.: Coordinating generation and load pickup during load restoration with discrete load increments and reserve constraints. IET Gener. Transm. Distrib. 9(15), 2437–2446 (2015)
18. Liu, X., et al.: Microgrids for enhancing the power grid resilience in extreme conditions. IEEE Trans. Smart Grid 8(2), 589–597 (2017)
19. Muhs, J.W., Parvania, M.: Stochastic spatio-temporal hurricane impact analysis for power grid resilience studies. In: 2019 IEEE Power & Energy Society Innovative Smart Grid Technologies Conference (ISGT), Washington, DC, USA, pp. 1–5 (2019)
20. Zhang, H., et al.: Spatial-temporal reliability and damage assessment of transmission networks under hurricanes. IEEE Trans. Smart Grid 11(2), 1044–1054 (2020)
21. Espinoza, S., et al.: Multi-phase assessment and adaptation of power systems resilience to natural hazards. Electr. Power Syst. Res. 136, 352–361 (2016)
22. Panteli, M., et al.: Power systems resilience assessment: Hardening and smart operational enhancement strategies. Proc. IEEE 105(7), 1202–1213 (2017)
23. Bektas, T., The multiple traveling salesman problem: An overview of formulations and solution procedures. Omega 34(3), 209–219 (2006)
24. Patsakis, G., et al.: Optimal black start allocation for power system restoration. IEEE Trans. Power Syst. 33(6), 6766–6776 (2018)
25. Jiang, Y., et al.: Blackstart capability planning for power system restoration. International Journal of Electrical Power & Energy Systems 86, 127–137 (2017)
26. Yang, Z., et al.: A linearized OPF model with reactive power and voltage magnitude: A pathway to improve the MW-only DC OPF. IEEE Trans. Power Syst. 33(2), 1734–1745 (2018)
27. Coffrin, C., Van Hentenryck, P.: A linear-programming approximation of AC power flows. INFORMS J. Comput. 26(4), 718–734 (2014)
28. Trodden, P.A., et al.: Optimization-based islanding of power networks using piecewise linear AC power flow. IEEE Trans. Power Syst. 29(3), 1212–1220 (2014)
29. Chen, X., et al.: Robust restoration method for active distribution networks. IEEE Trans. Power Syst. 31(5), 4005–4015 (2016)
30. Arif, A., et al.: Optimization of transmission system repair and restoration with crew routing. In: 2016 North American Power Symposium (NAPS), Denver, Colorado, pp. 1–6 (2016)
31. Rockafellar, R.T., Wets, R.J.-B.: Scenarios and policy aggregation in optimization under uncertainty. Math. Oper. Res. 16(1), 119–147 (1991)
32. Watson, J.P., Woodruff, D.L.: Progressive hedging innovations for a class of stochastic mixed-integer resource allocation problems. Comput. Manag. Sci. 8, 355–370 (2011)
33. Power systems test case archive–118 bus power flow test case. http://www2.ee.washington.edu/-research/pstca/pf118/pg_tca118bus.htm. Accessed 19 Nov 2019
34. Wang, D., et al.: Decision-making optimization of power system extended black-start coordinating unit restoration with load restoration. Int. Trans. Electr. Energy Syst. 27(1), 1–18 (2017)

How to cite this article: Bian Y, Bie Z, Li G. Proactive repair crew deployment to improve transmission system resilience against hurricanes. *IET Gener Transm Distrib.* 2021;15:870–882. https://doi.org/10.1049/gtd2.12065